Journal of Biomedical Optics

SPIEDigitalLibrary.org/jbo

On the sensitivity of thermophotonic lock-in imaging and polarized Raman spectroscopy to early dental caries diagnosis

Nima Tabatabaei
Andreas Mandelis
Mehdi Dehghany
Kirk H. Michaelian
Bennet T. Amaechi

SPIE

On the sensitivity of thermophotonic lock-in imaging and polarized Raman spectroscopy to early dental caries diagnosis

Nima Tabatabaei,[a] Andreas Mandelis,[a] Mehdi Dehghany,[b] Kirk H. Michaelian,[b] and Bennet T. Amaechi[c]
[a]University of Toronto, Center for Advanced Diffusion-Wave Technologies, Department of Mechanical and Industrial Engineering, Toronto, Ontario, M5S 3G8, Canada
[b]CANMET Energy Technology Centre-Devon, Natural Resources Canada, 1 Oil Patch Drive, Suite A202, Devon, Alberta, Canada T9G 1A8
[c]University of Texas Health Science Center at San Antonio, Department of Community Dentistry, San Antonio, Texas 78229-3900

Abstract. Dental caries is the leading cause of tooth loss, which can promptly be prevented if detected in early stages of progression. Unfortunately, conventional diagnostic modalities currently used in dentistry lack the sensitivity to detect early caries. The authors' intention is to compare the ability of polarized Raman spectroscopy and thermophotonic imaging to make early caries diagnosis. Extracted human teeth with no visible stain or defects were artificially demineralized in accordance to a well-known protocol in dentistry for simulated early caries development at several demineralization stages. Samples were then inspected using polarized Raman spectroscopy and thermophotonic imaging. The sensitivities of these two diagnostic modalities are compared, and the results are verified using transverse micro-radiography. It was found that compared to polarized Raman spectroscopy, thermophotonic imaging exhibits superior sensitivity to very early stages of demineralization. [DOI: 10.1117/1.JBO.17.2.025002]

Keywords: thermophotonic lock-in imaging; polarized Raman spectroscopy; dental caries; early caries detection; demineralization.

Paper 11539 received Sep. 23, 2011; revised manuscript received Dec. 6, 2011; accepted for publication Dec. 8, 2011; published online Feb. 23, 2012.

Dental caries is a chronic disease identified as the leading cause of tooth loss among children and adult populations. The precursor of the disease is a minute amount of mineral loss (demineralization) from the enamel surface as a result of decomposition of hydroxyapatite crystals in the acidic environment of dental plaque.[1] Given enough time, such early caries turns into a cavity, which requires surgical intervention. However, if the caries is detected early enough, not only can it be stopped (i.e., arrested) from progressing deeper into enamel, but also it can be healed (i.e., remineralized) using, for instance, oral hygiene counseling or fluoride therapy.[2,3] Unfortunately, conventional clinical diagnostic modalities lack sufficient sensitivity and/or specificity to detect early caries.[4] As a result, in the past two decades a surge of research has been focused on the development of technologies for early detection of dental caries. The majority of the proposed technologies are optics-based methods, which benefit from the intrinsic contrast associated with increased scattering of light within the early carious lesion. Polarized Raman spectroscopy (PRS), pioneered in dental caries diagnostics by Choo-Smith et al.,[5] is one such method that uses the degree of polarization in the backscattered light to differentiate between intact and carious enamel. Ko et al.[5] found that the increased porosity in early caries enhances light scattering and scrambles the polarization leading to larger depolarization of the Raman 960 cm^{-1} phosphate band of hydroxyapatite. This band in intact enamel preserves good polarization and returns smaller depolarization values.

Dental thermophotonic imaging (TPI), introduced by Tabatabaei et al.,[6,7] is another promising early caries detection method that incorporates intensity-modulated light to generate a thermal-wave field inside enamel and uses the subsequent infrared emission of the thermal-wave field to detect early dental caries. In this case, the increased light scattering of the early caries results in more light absorption and subsequently in enhanced heat generation, providing contrast between early caries and intact enamel.[6,7] Unlike purely optical methods, such as PRS, TPI is based on energy conversion between optical and thermal fields, where excitation is optical but detection is thermal. As a result, TPI is insensitive to any kind of radiation outside the spectral range of the mid-infrared camera (3 to 5 μm). Despite promising results of PRS no studies have been reported on the sensitivity of this method to the amount of demineralization using conventional controlled demineralization protocols followed by verification through dental gold standards, such as transverse micro-radiography (TMR). The intention of this paper is to provide a comparison between the ability of PRS and TPI in detecting very early dental caries.

The sensitivity of polarized Raman spectroscopy and thermophotonic imaging to early caries detection was investigated using two relatively healthy extracted human teeth without any stain or surface defects, labeled samples S1 and S2. The samples were carefully cleaned and mounted on Lego blocks. Mounting the teeth on Lego blocks allowed their remounting into the same position in the experimental setup during repeated measurements. The surfaces of the samples were neither polished nor

Address all correspondence to: Andreas Mandelis, University of Toronto, Center for Advanced Diffusion-Wave Technologies, Department of Mechanical and Industrial Engineering, Toronto, Ontario, M5S 3G8, Canada. Tel: +416/978 5106; Fax: +416/266 7867; E-mail: mandelis@mie.utoronto.ca

0091-3286/2012/$25.00 © 2012 SPIE

altered in any way prior to the experiments. In order to apply controlled demineralization on samples, a demineralizing solution was prepared. The solution was an acidified gel, consisting of 0.1 M lactic acid gelled to a thick consistency with 6% w/v hydroxyethylcellulose and the pH adjusted to 4.5 with 0.1 M NaOH. Demineralization with acidified gel approximates the natural lesion as it mimics the properties of actual dental plaque in the oral cavity.[8] Our previous studies show that this solution can produce a subsurface lesion in enamel with a sound surface layer, a characteristic of early caries.[6,7,9] To see the contrast between early caries and the surrounding healthy areas, the interrogated surface of the sample was covered with two coatings of commercial transparent nail polish except for rectangular windows, henceforth referred to as treatment windows [Fig. 1(c)]. Sample S1 had two treatment windows on the interrogated surface while sample S2 had only one treatment window. The demineralization on the windows was carried out by submerging the samples upside down in a polypropylene test tube containing 30 ml of demineralizing solution. The left and right treatment windows of S1, Fig. 1(c), were treated for two and four days, respectively, and that of S2, Fig. 1(e), was treated for 20 days. After the treatment the transparent nail polish was removed from the interrogated surfaces with acetone, and inspection was carried out using our thermophotonic imaging and polarized Raman spectroscopy systems.

The thermophotonic experimental setup was built using a continuous-wave fiber-coupled 808-nm near-infrared (NIR) laser illuminating the sample (JENOPTIK, Germany) with beam size of 20 mm and a fluence of 2 W/cm^2, a mid-infrared camera focused on the interrogated surface of the sample (Cedip Titanium 520 M, France, spectral range of 3.6 to 5.1 μm and frame rate of 360 Hz), a signal generation/acquisition device (National Instruments NI-6229 BNC), and a 4-axis sample positioning system, Fig. 1(a).[6] The laser power was modulated sinusoidally by the signal generation device at 1 Hz to generate photothermal waves inside the sample. The data acquisition/signal processing program (designed in LabView environment) captured and averaged the camera frames and their corresponding reference/modulation signal values. Finally, amplitude and phase images were calculated using a standard 2D quadrature demodulation of the camera data as graphically shown in Fig. 1(b).[6]

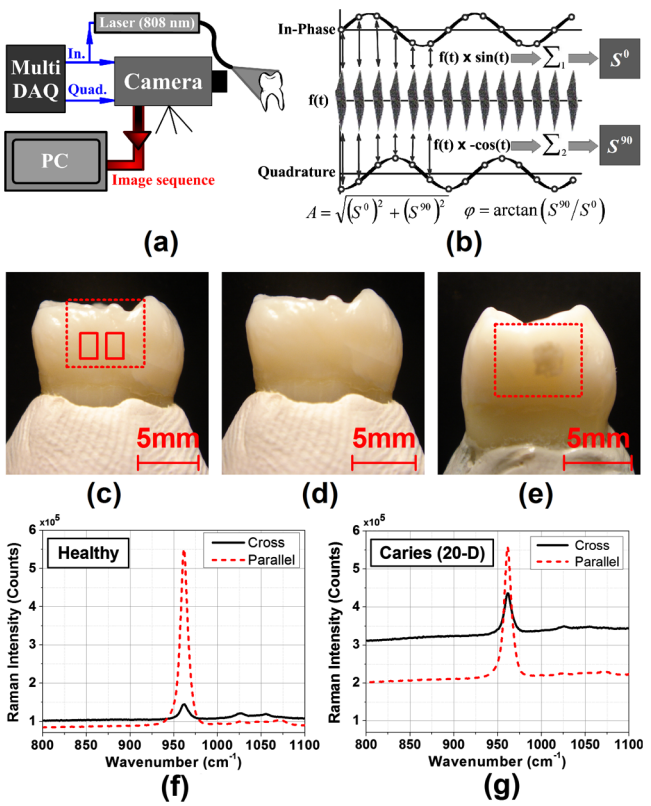

Fig. 1 Schematic representation of (a) thermophotonic imaging setup and (b) its signal processing algorithm. Photographs of S1 (c) before and (d) after the demineralization treatment. (e) Photograph of sample S2 after the treatment. The dotted and solid rectangles show the imaged area and the locations of the treatment windows. The cross (solid) and parallel (dashed) Raman spectra of (f) a healthy spot on S1 and (g) the 20-day-treated caries in sample S2.

Raman spectra of the tooth samples were acquired using a fully automated Renishaw inVia confocal Raman microspectrometer. Excitation was provided by a linearly polarized 633-nm Spectra Physics He-Ne laser with an output power of 30 mW and beam size of 1×1 mm^2 yielding an optical fluence of 3 W/cm^2 at the laser output. In this system, a set of mirrors, positioned on automated stages, directs the laser beam to the microscope compartment where a Raman excitation spot size of approximately 50 μm is obtained through a 50× objective lens. Scattered light is collected using a 180-deg backscattering geometry and directed to an optical notch filter that eliminates the intense Rayleigh scattering. A rotary stage holds a half-wave plate (HWP) and an analyzer in the beam path at normal incidence; these components are used to determine the polarization characteristics of the Raman spectra of tooth enamel. The scattered light is dispersed by an 1800 line/mm holographic diffraction grating and focused on a CCD camera with a concave lens.

Parallel- and cross-polarized components of the scattered light were recorded at a series of points on the enamel of the tooth samples. The HWP was employed only for the parallel polarization measurements. All spectra were recorded using 50% of the available laser power, with a 50-s acquisition time and five accumulations. The Raman band at 960 cm^{-1}, due to the totally symmetric phosphate (PO_4^{3-}) vibration within hydroxyapatite, exhibits strong polarization dependence; accordingly spectra were acquired only in the 800 to 1100 cm^{-1} range, as shown in Figs. 1(f) and 1(g). Peak intensities were obtained by numerically fitting the data to Lorentzian functions. Several experiments showed that the background intensity in the spectra has negligible effects on the parallel-/cross-polarization intensity ratios for healthy and demineralized enamel.

The use of short laser wavelengths in Raman spectroscopy sometimes gives rise to significant fluorescence backgrounds that mask weak Raman bands. In this work the 633 nm excitation yielded acceptable backgrounds which did not adversely affect intensity measurements. Specifically, baseline effects were minimal as there were no stains on the samples and therefore the capability of Raman spectroscopy with regard to caries detection was not affected.[10] This wavelength is slightly shorter than that used in the thermophotonic system, an advantage in PRS since the intensity of Raman scattering is inversely proportional to the fourth power of excitation wavelength ($\propto 1/\lambda^4$).

Figure 2 represents the thermophotonic phase images of S1 and S2 before and after the treatment using identical linear contrast mapping. Figures 2(a) and 2(b) show that even before applying the artificial demineralization, thermophotonic imaging can sense the inhomogeneities of the sample. The phase image of S1 after the treatment, Fig. 2(c), clearly reveals the

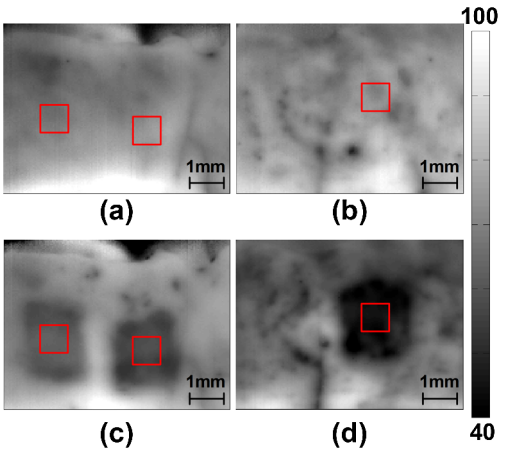

Fig. 2 Thermophotonic phase images of (a) S1 and (b) S2 before demineralization treatment and (c) S1 and (d) S2 after treatment using the linear contrast mapping shown in the figure. The squares (20×20 pixels) indicate the regions used for statistical analysis.

two- (left) and four- (right) day-treated windows, 2-D and 4-D, respectively, which are not visible in the visual photograph of Fig. 1(d). The phase values at the center of the 2-D and 4-D regions [indicated by the squares in Fig. 2(c)] were found to be 61.64 ± 1.23 deg and 57.89 ± 1.17 deg, respectively, while the phase values at the exact same regions before treatment (i.e., healthy) were measured to be 71.05 ± 3.96 deg [indicated by the squares in Fig. 2(a)]. Such a good contrast between the intact and infinitesimally demineralized enamel comes from the way light interacts with enamel. Intact enamel is semi-transparent to NIR radiation, and as a result, light is gradually absorbed as it penetrates deeply into the enamel, yielding a thermal-wave field with a deep centroid (large phase values). Demineralization, on the other hand, always starts from the enamel surface and replaces the hydroxyapatite crystals of this close-to-surface enamel with micro-cavities, increasing light scattering and absorption near the surface and therefore shifting the thermal-wave centroid towards the surface, yielding smaller phase values. Therefore, the mean phase value of the 20-day-treated window (20-D), Fig. 2(d), was found to be smaller than those of 2-D and 4-D regions (44.50 ± 0.93 deg) as the additional treatment days resulted in more light absorption closer to the enamel surface.

Figures 1(f) and 1(g) are plots of the cross and parallel polarized Raman spectra of healthy and carious spots on S2, respectively. According to the literature,[5,11,12] the dominant Raman band is the 960 cm^{-1} phosphate band (PO stretching) of hydroxyapatite. Previous studies have shown that this band is the most sensitive Raman band to the structural changes on dental enamel during early demineralization. Moreover, the Raman spectra of healthy and 20-D regions clearly show that the fluorescence background was not high enough to obscure the PO band, as the samples were artificially demineralized and no stain was present on the surface.[10] While the Raman response of the healthy enamel, Fig. 1(f), preserves the polarization of the applied excitation, the increased scattering of caries scramble the polarization and yields dominant 960 cm^{-1} bands in both parallel and cross spectra, Fig. 1(g). Consequently, as suggested by Ko et al.,[5] one can use the Raman depolarization ratio of the 960 cm^{-1} band, $\rho_{960,}$, to monitor the structural changes of enamel:

$$\rho_{960} = I_{\perp}/I_{\parallel}, \tag{1}$$

where $I_{\parallel}$ and $I_{\perp}$ are the peak to fluorescence baseline intensity of the 960 cm^{-1} band in the parallel and cross spectra, respectively. However, the question remains as to how sensitive the ρ_{960} is to the early structural changes in enamel. The bar plot of Fig. 3(a) represents the mean ρ_{960} obtained from S1 and S2 along with the standard deviation of these measurements over the healthy, 2-D, 4-D, and 20-D regions. The number next to each error bar depicts the number of Raman experiments carried out on that region. The 47 Raman measurements suggest that one cannot statistically differentiate the 2-D and 4-D treatment windows from healthy areas, nor can one garner any statistical difference between the 2-D and 4-D early caries. However, the well-developed 20-D caries of S2 is detectable by polarized Raman spectroscopy. In analogy to Fig. 3(a), the bar plot of Fig. 3(b) shows the mean thermophotonic phase values and their standard deviations over the regions of interest in S1 and S2 (shown by the squares in Fig. 2). It can be seen that the phase value decreases as more mineral is removed from enamel to manifest the shifting of the thermal-wave centroid towards the interrogated surface of enamel. Moreover, it can be seen that thermophotonic imaging can reliably differentiate between the healthy, 2-D, 4-D, and 20-D regions. Consequently, the bar plots suggest that polarized Raman spectroscopy is not sensitive enough to detect the onset or the very early stages of demineralization while thermophotonic imaging can reliably detect it. The reason for the enhanced sensitivity of thermophotonic imaging is the fact that, unlike Raman spectroscopy, this form of detection belongs to the group of energy conversion methodologies with reduced signal baseline and enhanced dynamic range advantages where one excites optically and detects thermally whereas in Raman spectroscopy excitation and detection are both optical. Finally, Fig. 3(c) shows the TMR profiles obtained at the center of the artificial caries created in S1 and S2 as the verification of the comparison made in this paper. It can be seen that both of the artificially

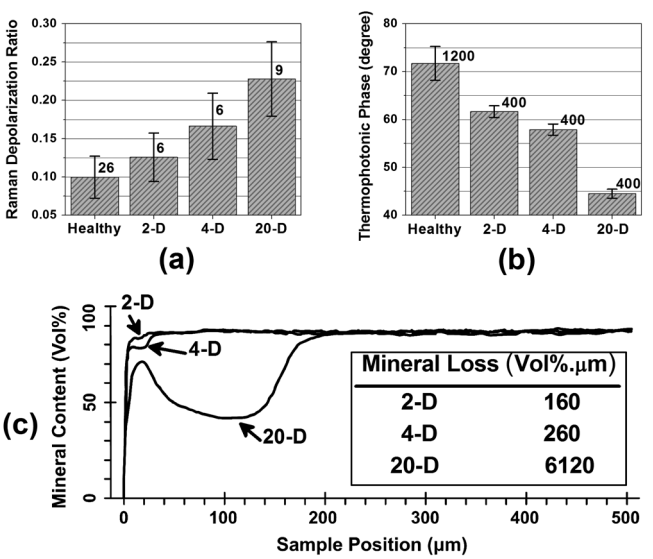

Fig. 3 The mean (a) Raman depolarization ratio and (b) thermophotonic phase values obtained in healthy, 2-D, 4-D, and 20-D regions of samples S1 and S2 along with their standard deviations. (c) The mean transverse micro-radiography mineral profiles of 2-D, 4-D, and 20-D treatment windows.

generated caries of S1 are truly in the initial stages of formation when they can easily get arrested and remineralized, but the caries in S2 has undergone a gigantic mineral loss near the surface, which may even be detected by visual inspection, Fig. 1(e).

In conclusion, using a well-known controlled dental demineralization protocol, we have compared the sensitivity of polarized Raman spectroscopy and thermophotonic lock-in imaging to the structural changes of early enamel caries. Our results show that polarized Raman spectroscopy cannot reliably detect the onset of early caries, while thermophotonic imaging not only can detect such early structural changes, but also images the extent of the caries with high contrast. The results are verified by destructive transverse micro-radiography mineral profiles.

Acknowledgments

We are grateful to the Ontario Ministry of Research and Innovation (MRI) for the 2007 (inaugural) Discovery Award in Science and Engineering to A. M., to the Canada Research Chairs Programs, the Federal and Provincial Governments for a CFI-ORF award and the Natural Sciences and Engineering Research Council of Canada for several Discovery Grants to A. M.

References

1. J. M. Ten Cate et al., "Chemical interactions between the tooth and oral fluids," Chapter 4 in *Dental Caries: The Disease and its Clinical Management*, O. Fejerskov and E. Kidd, Eds., pp. 49–70, 3rd ed., Blackwell Munksgaard, Carlton, Australia (2004).
2. J. D. B. Featherstone, "Prevention and reversal of dental caries: role of low level fluoride," *Commun. Dent. Oral.* **27**(1), 31–40 (1999).
3. M. Fontana, D. A. Young, and M. S. Wolff, "Evidence-based caries, risk assessment, and treatment," *Dent. Clin. N. Am.* **53**(1), 149–161 (2009).
4. S. C. White and M. J. Pharoah, "Dental caries," in *Oral Radiology: Principles and Interpretation*, 5th ed., Mosby, Toronto, pp. 297–313 (2004).
5. A. C. T. Ko et al., "Detection of early dental caries using polarized Raman spectroscopy," *Opt. Express* **14**(1), 203–215 (2006).
6. N. Tabatabaei, A. Mandelis, and B. T. Amaechi, "Thermophotonic lock-in imaging of early demineralized and carious lesions in human teeth," *J. Biomed. Opt.* **16**(7), 0714021–07140210 (2011).
7. N. Tabatabaei, A. Mandelis, and B. T. Amaechi, "Thermophotonic radar imaging: an emissivity-normalized modality with advantages over phase lock-in thermography," *Appl. Phys. Lett.* **98**(16), 163706 (2011).
8. N. W. Johnson, "Differences in the shape of human enamel crystallites after partial destruction by caries, EDTA and various acids," *Arch. Oral. Biol.* **11**(12), 1421–1424 (1966).
9. R. J. Jeon et al., "In vitro detection and quantification of enamel and root caries using infrared photothermal radiometry and modulated luminescence," *J. Biomed. Opt.* **13**(3), 0340251–03402511 (2008).
10. J. Li et al., "Background removal from polarized Raman spectra of tooth enamel using wavelet transform," *J. Raman Spectrosc.* **42**(4), 580–585 (2011).
11. E. Yokoyama, S. Kakino, and Y. Matsuura, "Raman imaging of carious lesions using a hollow optical fiber probe," *Appl. Opt.* **47**(23), 4227–4230 (2008).
12. H. Kinoshita et al., "Functional mapping of carious enamel in human teeth with Raman microspectroscopy," *J. Raman Spectrosc.* **39**(5), 655–660 (2008).